Nonlinear and Adaptive Estimation in Re-Entry

ANDREW H. JAZWINSKI*
Business and Technological Systems Inc., Seabrook, Md.

The problem of real-time estimation of a lifting re-entry vehicle trajectory of the shuttle orbiter type is considered. Two distinct estimation algorithms are presented and simulated in the re-entry problem. Simulations feature large position and velocity uncertainties at radar acquisition and realistic model errors in lift, drag and other model parameters. Radar tracking and accelerometer data are simulated. Significant nonlinearities are found to exist on spacecraft acquisition. An iterated nonlinear filter is shown to perform optimally during the radar acquisition phase. An adaptive filter is shown to track time-varying model errors, such as errors in the lift and drag coefficients, down to the noise level. Such real-time model tracking (identification) is frequently required for guidance and control implementation.

I. Introduction

THIS paper deals with the development and simulation of nonlinear and adaptive estimators for re-entry (e.g., space shuttle) navigation and model parameter estimation or identification. Of particular interest is the identification of vehicle lift and drag characteristics in real time, since these are important for guidance and control applications. Published work in re-entry estimation[1] indicates the importance of nonlinear effect in re-entry trajectory estimation. In post flight trajectory reconstruction, batch least squares methods tend to diverge, and the standard extended Kalman filter appears unsuitable for real-time applications. This motivates the application of nonlinear filtering techniques[2] to the re-entry problem. Some related work on ballistic re-entry trajectory estimation may be found in Ref. 3.

Several nonlinear filters are simulated in the re-entry problem. In addition, adaptive filters for the real-time identification of vehicle lift and drag characteristics, and unmodelable acceleration, are developed and tested by simulation. The simulations feature an uncertain system environment with rather arbitrary model errors, thus providing a definitive test of estimator performance.

It is found that nonlinear effects can be significant in re-entry trajectory estimation and a nonlinear filter is demonstrated which successfully tracks through nonlinearities without degrading the information content of the data. Under the same conditions, the usual extended Kalman filter diverges and is useless. Interesting relationships are also found between nonlinearities and tracking geometry. The J-adaptive filter is shown to successfully track errors in the modeled vehicle lift and drag characteristics. The same filter concept is also shown to track successfully through rather arbitrary model errors, including lift and drag errors, vehicle mass errors, atmospheric density errors and wind gusts.

II. The System and System Model

The vehicle translation motion is described in an inertial (geocentric) rectangular coordinate system. The Earth is assumed to be oblate and rotating. Forces acting on the vehicle consist of gravity, lift and drag. If R is the vehicle (c.g.) position vector, then the motion is described by

$$\ddot{R} = g + (L+D)/m \tag{1}$$

where g is the gravitational acceleration vector, L and D are the lift and drag vectors, respectively, and m is the vehicle mass. It is assumed that vehicle turns are coordinated, so that a side force is only produced by a rotation of the lift vector around the relative velocity vector. The details of the characterization of L and D in inertial coordinates, as well as other model details, may be found in Ref. 4. The model includes atmospheric density as a tabulated function of altitude; lift and drag coefficients $C_L(\alpha, M)$, $C_D(\alpha, M)$ as tabulated functions of angle of attack and Mach number; and the speed of sound as a tabulated function of altitude. East and north wind components are also provided in the model.

The measurement system consists of radar tracking and onboard linear accelerations. Radar tracking consists of range, azimuth and elevation measurements from several tracking stations; accelerations along the three inertial axes are measured. Measurements are sampled at discrete time instants.

We make a distinction between what we shall call the real system and the system model. Differences between the two are shown in Table 1 and consist of different constants for the oblateness coefficient J_2 and mass m, different density profiles and different wind (time) functions in the east and north wind components w_E and w_N, and different lift and drag coefficient models as indicated in Table 1. The real system is used to generate measurements which are then processed by a filter based on the system model.

Estimators are designed on the basis of the system model. We always estimate the position R and velocity V of the vehicle. To this end we define the 6-dimensional state vector x

$$x^T = [x_1 x_2 x_3 \vdots x_4 x_5 x_6] = [R^T \vdots V^T] \tag{2}$$

Sometimes we estimate errors in the lift and drag coefficients ΔC_L and ΔC_D. In that case we can define the 2-vector

$$u = \begin{bmatrix} \Delta C_L \\ \Delta C_D \end{bmatrix} \tag{3}$$

Table 1 Real and model systems

Real system	System model
J_2 Real	J_2 Model
m Real	m Model
ρ Real	ρ Model $= \rho$ Real $(1+k_1)$
w_E, w_N Real	w_E, w_N Model $= w_E$, w_N Real $+\Delta w_E$, Δw_N
C_L Real	C_L Model $= C_L$ Real $+ C_{L\alpha}\alpha$
C_D Real	C_D Model $= C_D$ Real $+ C_A + \eta_1\alpha + \eta_2\alpha^2$
k_1, $C_{L\alpha}$, C_A, η_1, η_2 const	

Presented as Paper 72-874 at the AIAA Guidance and Control Conference, Stanford, Calif., August 14–16, 1972; submitted August 1, 1972; revision received January 24, 1973. This research is supported by NASA/MSFC Dynamics and Control Division under contract NAS-8-26973.

Index categories: Navigation, Control, and Guidance Theory; Spacecraft Tracking; Entry Vehicle Dynamics and Control.

* President. Member AIAA.

and modify the dynamical Eq. (1) by replacing C_L and C_D by

$$C_L+u_1, \qquad C_D+u_2 \tag{4}$$

and take the resulting equation as our model. When we estimate unknown (or unmodeled) accelerations we define a 3-vector u to represent these unknown accelerations. In this case u is added to the right-hand side of Eq. (1) and the resulting equation is taken as our model. The modeled acceleration measurement equations are also appropriately modified.

Let $f(\cdot)$ be the 6-vector mapping defined by Eq. (1), with the system model parameters as given in Table 1. Then the system dynamical model is given by

$$x(i+1)=f[x(i), u(i)]+w(i) \tag{5}$$

where u is either a 2-vector of C_L and C_D errors [Eq. (3)], or a 3-vector of unknown accelerations. w is a 6×1 vector of zero-mean, white gaussian noise inputs.

The re-entry trajectory used in simulations, as well as the vehicle aerodynamic characteristics are described in detail in Ref. 4, and are not included here because of space limitation. The vehicle simulated is a delta orbiter with a hypersonic (L/D)max of 2.3 and subsonic (L/D)max of 5.3. The vehicle weighs 245,703 lb and has a reference area of 5990 ft^2. The re-entry is three dimensional from essentially a polar orbit of about 120 km alt (Mach number 28) to about 15 km alt (Mach number <1). The trajectory contains several skips (mentioned here because they correlate with state uncertainties).

All simulations (Secs. V–VII) are performed with a diagonal initial estimation error covariance matrix, with a standard deviation of 3 km in the position components and 150 m/sec in the velocity components. Actual errors in the initial position and velocity estimate are consistent with these statistics. These errors are sizable, but probably realistic at spacecraft acquisition. Radar tracking is simulated from several tracking stations. During radar coverage a 3-vector measurement of range, azimuth and elevation is processed every 4 sec. The noise standard derivations in these measurements are

$$\sigma(\text{range})=3\,\text{m}, \qquad \sigma(\text{azimuth})=\sigma(\text{elevation})=0.01^\circ \tag{6}$$

When simulated, accelerations are processed as a 3-vector measurement every 4 sec. The noise standard deviation in each acceleration component is

$$\sigma(\text{accel})=0.002\,(\text{accel})+10^{-6}\,\text{km/sec}^2 \tag{7}$$

The estimators (filters) simulated as usual require a system state transition matrix (see Secs. III and IV). Approximate closed form expressions for the state transition matrix have been successfully utilized in the re-entry problem. The interested reader may find the details of these approximations in Refs. 4 and 5.

III. Nonlinear Filters

Several nonlinear filters are presented in Refs. 2 and 4, and Ref. 4 describes simulation results for these filters. Here we describe one such filter (the iterated extended Kalman filter), and present simulation results for this filter in Sec. V. We assume the reader is familiar with the usual extended Kalman filter.[2]

The basic system model for the nonlinear filter is given by

$$x(i+1)=f[x(i)]+w(i) \qquad y(i)=h[x(i)]+v(i) \tag{8}$$

where x is the state vector and y the measurement vector. $w(i)$, $v(i)$ are independent, zero-mean, white gaussian noise sequences with

$$\mathscr{E}[w(i)w^T(i)]=Q(i) \qquad \mathscr{E}[v(i)v^T(i)]=R(i) \tag{9}$$

Estimators in general involve recursions for the estimate of the state ($\hat{x}$) and the estimation error covariance matrix (P). $\hat{x}(i\,|\,j)$ is the estimate of the state at time t_i, and $P(i\,|\,j)$ is the estimation error covariance matrix at time t_i, given all measurements up to and including time t_j.

The extended Kalman filter is iterated at each measurement to improve the reference trajectory and thus also the estimate (see Ref. 2 p. 279). The iteration involves only the estimate update equation; that equation is replaced by the iteration

$$\eta_{k+1}=\hat{x}(i\,|\,i-1)+K(i,\eta_k)\{y(i)-h(\eta_k)-M(i,\eta_k)[\hat{x}(i\,|\,i-1)-\eta_k]\} \qquad k=1,\ldots,l \tag{10}$$

where K is the Kalman gain and M is the matrix of partials of the measurement function h with respect to the state x. The iteration starts with

$$\eta_1=\hat{x}(i\,|\,i-1) \tag{11}$$

and we set

$$\hat{x}(i\,|\,i)=\eta_l \tag{12}$$

Observe that the gain K, matrix M, and function h are recomputed each iteration (evaluated at iterate η_k). The covariance matrix $P(i\,|\,i)$ is computed only after the iteration has converged. Note that the second iterate, η_2, is merely the output of the usual extended Kalman filter. This iteration has a probabilistic (maximum likelihood) interpretation which may be found in Chap. 9, Sec. 7 of Ref. 2.

IV. The J-Adaptive Filter

The adaptive filter to be described is designed to track time-varying model errors. Thus, in one instance, the filter tracks the 2-vector u of lift and drag errors [Eq. (3)], and in the second instance it tracks a 3-vector u of unmodeled accelerations. To this end, we take the system model given by

$$\begin{gathered} x(i+1)=f[x(i), u(i)]+w(i), \qquad u(i+1)=u(i) \\ y(i)=h[x(i), u(i)]+v(i) \end{gathered} \tag{13}$$

where u is a random (unknown) forcing function to be estimated. In order to track unpredictable variation in u with the above model, we maintain the uncertainty in u constant (or some specified function which does not decrease as a result of the estimation process). That is

$$\mathscr{E}\{[u(i)-\hat{u}(i\,|\,j)][u(i)-\hat{u}(i\,|\,j)]^T\}=U \tag{14}$$

where the covariance matrix U is specified.

The J-adaptive filter is derived by augmenting the state x with u, writing the augmented filter in partitioned form, and discarding the equations for the covariance matrix U. This exercise is given on pp. 281–286 of Ref. 2. To write the result, we need, in addition to the state estimation error covariance matrix $P(i\,|\,j)$,

$$P(i\,|\,j)=\mathscr{E}\{[x(i)-\hat{x}(i\,|\,j)][x(i)-\hat{x}(i\,|\,j)]^T\} \tag{15}$$

the following correlation matrix

$$C_u(i\,|\,j)=\mathscr{E}\{[x(i)-\hat{x}(i\,|\,j)][u(i)-\hat{u}(i\,|\,j)]^T\} \tag{16}$$

The J-adaptive filter is then given by

$$\begin{aligned} &\hat{x}(i+1\,|\,i)=f[\hat{x}(i\,|\,i), \hat{u}(i\,|\,i)] \qquad \hat{u}(i+1\,|\,i)=\hat{u}(i\,|\,i) \\ &P(i+1\,|\,i)=\Phi(i+1,i)P(i\,|\,i)\Phi^T(i+1,i)+ \\ &\quad \Phi(i+1,i)C_u(i\,|\,i)\Psi^T(i+1,i)+ \\ &\quad \Psi(i+1,i)C_u{}^T(i\,|\,i)\Phi^T(i+1,i)+ \\ &\quad \Psi(i+1,i)U\Psi^T(i+1,i)+Q(i) \end{aligned} \tag{17}$$

$$\begin{aligned} &C_u(i+1\,|\,i)=\Phi(i+1,i)C_u(i\,|\,i)+\Psi(i+1,i)U, \quad C_u(0\,|\,0)=0 \\ &\hat{x}(i\,|\,i)=\hat{x}(i\,|\,i-1)+K_x(i)[y(i)-h(\hat{x}(i\,|\,i-1), \hat{u}(i\,|\,i-1))] \\ &\hat{u}(i\,|\,i)=\hat{u}(i\,|\,i-1)+K_u(i)[y(i)-h(\hat{x}(i\,|\,i-1), \hat{u}(i\,|\,i-1))] \\ &P(i\,|\,i)=P(i\,|\,i-1)-K_x(i)[M(i)P(i\,|\,i-1)+N(i)C_u{}^T(i\,|\,i-1)] \\ &C_u(i\,|\,i)=C_u(i\,|\,i-1)-K_x(i)[M(i)C_u(i\,|\,i-1)+N(i)U] \end{aligned} \tag{18}$$

where

$$\begin{aligned} &K_x(i)=[P(i\,|\,i-1)M^T(i)+C_u(i\,|\,i-1)N^T(i)]\,Y^{-1}(i) \\ &K_u(i)=[C_u{}^T(i\,|\,i-1)M^T(i)+UN^T(i)]Y^{-1}(i) \\ &Y(i)=M(i)P(i\,|\,i-1)M^T(i)+M(i)C_u(i\,|\,i-1)N^T(i)+ \\ &\quad N(i)C_u{}^T(i\,|\,i-1)M^T(i)+N(i)UN^T(i)+R(i) \end{aligned} \tag{19}$$

and

$$\begin{aligned} &\Phi(i+1,i)=\left.\frac{\partial x(i+1)}{\partial x(i)}\right|_{\hat{x}(i\,|\,i),\,\hat{u}(i\,|\,i)}, \qquad \Psi(i+1,i)=\left.\frac{\partial x(i+1)}{\partial u(i)}\right|_{\hat{x}(i\,|\,i),\,\hat{u}(i\,|\,i)} \\ &M(i)=(\partial h/\partial x)|_{\hat{x}(i\,|\,i-1),\,\hat{u}(i\,|\,i-1)} \\ &N(i)=(\partial h/\partial u)|_{\hat{x}(i\,|\,i-1),\,\hat{u}(i\,|\,i-1)} \end{aligned} \tag{20}$$

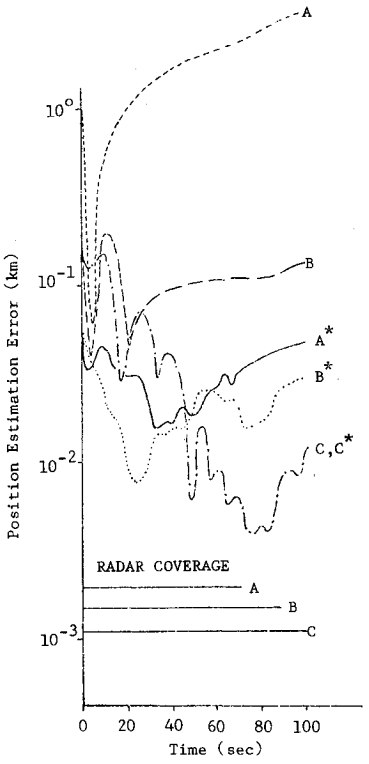

Fig. 1 Acquisition phase.

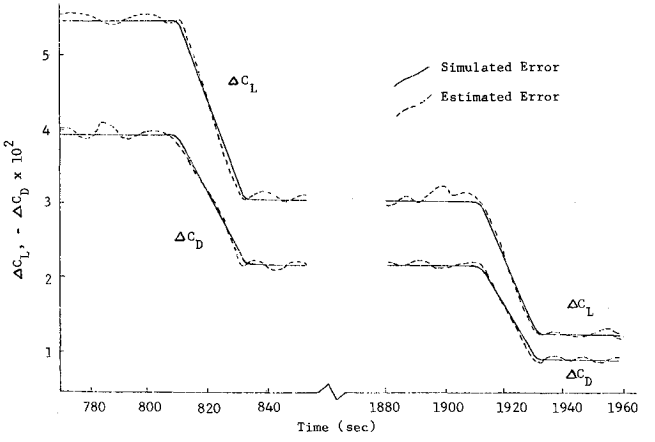

Fig. 2 Estimation of lift and drag errors.

V. Estimation in the Presence of Nonlinearities

The iterated extended Kalman filter was simulated in a perfect model environment (with no process noise) in order to study nonlinear effects in the re-entry problem. Under certain conditions dramatic nonlinear effects are observed. A description of the re-entry trajectory initial conditions, noise standard derivation, etc., may be found in Sec. II.

Figure 1 shows a sample time history of position estimation errors ($|R-\hat{R}|$) for the usual extended Kalman and the iterated extended Kalman filters during a pass over the first tracking station. This simulation involves tracking only; acceleration measurements appear to have insignificant effect on these results. A family of curves is presented, depending on the line of sight elevation angle (E_0) at spacecraft acquisition (acquisition angle). Curves A, B and C are the errors for the extended Kalman filter, while curves A^*, B^*, C^* are the errors for the iterated extended Kalman filter. Curves A and A^* correspond to $E_0 = 78.3°$, curves B and B^* correspond to $E_0 = 44.6°$, and curves C, C^* correspond to $E_0 = 14°$. It is seen that the extended Kalman filter diverges for high acquisition angles while the iterated extended Kalman filter performs well. At low acquisition angles both filters perform similarly and well. The fact that the estimates are generally better after 65 sec for lower acquisition angles is due to longer duration of radar coverage, as indicated in the figure. Similar results hold for velocity estimation errors.

These results have the following interpretation. At high acquisition angles information rates and nonlinearities are high, calling for relatively large corrections. The extended Kalman filter, designed for linear or nearly linear systems, when called upon to make large corrections, fails and is useless. We apparently have a filter (the iterated extended Kalman filter) capable of tracking under these conditions.

At low acquisition angles information rates are low, calling for smaller corrections, and under these conditions the extended Kalman filter works well. It is to be noted that the covariance matrix of the iterated extended Kalman filter is consistent with its estimation errors, while for the extended Kalman filter it is not. In the latter case errors are orders of magnitude larger than those predicted by the covariance matrix.

An interesting and very significant feature of these results is the fact that the covariance matrices associated with the two filters are the same, to almost two significant digits. This means that linearized error analyses produce good results for the present problem, but, such error analyses are indicative of the performance of an optimal filter, not of the standard extended Kalman filter. To put it another way, if one has in mind the usual filter, linearized error analysis is wrong, misleading and optimistic. If one has in mind an optimal filter, the error analysis is correct. Our simulations indicate that, in the present case, we have such an optimal filter.

To summarize briefly, these results have significant implications for 1) filter design, 2) tracking station (or beacon) placement and tracking schedule design, and 3) error analyses interpretations for re-entry trajectory estimation.

It is to be noted that the nonlinear effects seen in Fig. 1 can only be observed during transients when position and velocity uncertainties are relatively high (e.g., acquisition). When extended Kalman filter C encounters the next tracking station at a high acquisition angle, then, provided its errors are low, its performance will be satisfactory. Whether or not its errors will be low at the next station acquisition depends on the length of the data gap. It pays to iterate when uncertainties and information rates are both high. Once uncertainties are brought down, the iteration can be stopped. After approximately 30 sec, the iteration in filter A^* is unnecessary.

Now the divergence of filters A and B can be avoided by adding process noise to the filter. While divergence can thus be avoided, such a filter will clearly have poorer performance than the iterated filter since the system model is then more uncertain. This will result in a large covariance matrix and consequently noisier estimates. Similar comments apply to the artifice of increasing the measurement noise covariance matrix R, a device sometimes successfully used to prevent filter divergence. The iterated extended Kalman filter directly addresses and solves the problem of nonlinearities in the present situation.

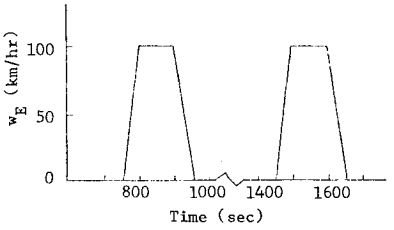

Fig. 3 East wind component.

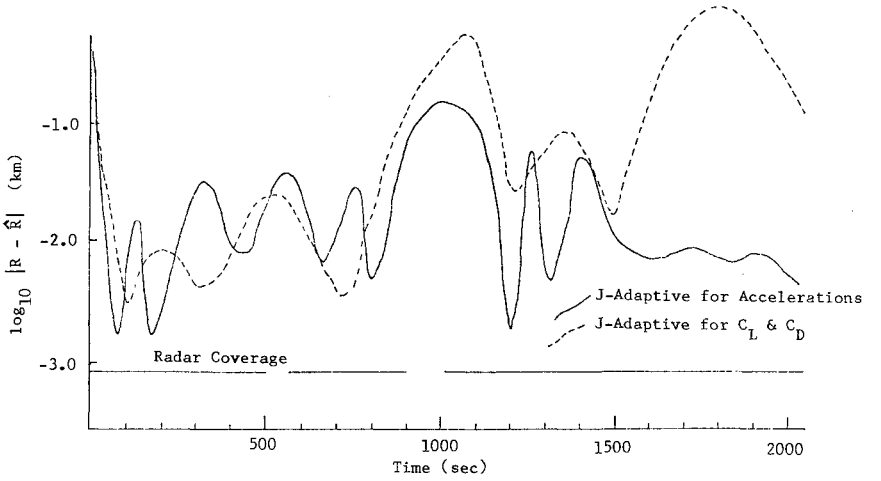

Fig. 4 Position estimation errors.

VI. Identification of Lift and Drag

One of the more important problem areas in atmospheric trajectory estimation is the lack of precise knowledge of the dynamical model. Thus it may be necessary to estimate in real time certain model parameters, and it can be expected that these parameters or parameter errors will be time-varying. Such estimation is important not only for the trajectory estimation or navigation, but also for guidance and control, which can depend on such parameters. In particular, the model for lift and drag coefficients of the vehicle can be uncertain and, for guidance and control purposes, it may be necessary to estimate such errors in real time.

Errors in the lift and drag models were simulated by setting $C_{L\alpha} = 0.07$, $C_A = 0$, $\eta_1 = -0.05$, $\eta_2 = 0$ (see Table 1). The resulting errors represent approximately 10% of the real lift and drag coefficients. Figure 2 shows the performance of the J-adaptive filter for lift and drag coefficients in estimating these lift and drag errors. The simulated error and its estimate via the J-adaptive filter is plotted. The filter was simulated with a diagonal matrix U with elements $U_{11} = (1.0 \times 10^{-2})^2$ and $U_{22} = (6.0 \times 10^{-3})^2$; $Q = 0$. Tracking and onboard accelerations were used in this simulation.

It is seen from the sample simulation in Fig. 2 that the J-adaptive filter tracks these errors extremely well. The error remaining after the estimation is always less than 5% of the simulated error or less than 0.5% of the real lift and drag coefficients; and usually substantially less than this. It should be noted that the filter is not very sensitive to the choice of the matrix U. The position and velocity estimation errors associated with this simulation are not shown here for lack of space. Their general features are similar to Figs. 4 and 5 which are described in Sec. VII. The discussion of Sec. VII is also generally applicable here.

VII. Estimation in the Presence of Arbitrary Model Errors

Several filters are simulated in the presence of arbitrary or unmodelable errors. The errors simulated include the 10% C_L and C_D errors described in the preceding section. In addition, errors in vehicle mass, atmospheric density and unmodeled winds are simulated. With reference to Table 1, m (real) = 111,448 kg, while m (model) = 112, 562 kg. This represents a 1% error in vehicle mass. Density errors are simulated with $k_1 = 0.03$. This represents a 3% error in atmospheric density. The simulated east wind is shown in Fig. 3 ($w_N = 0$). On the other hand, $\Delta w_E = -w_E$ and $\Delta w_N = -w_N$, so that the system model has no winds.

The filters simulated are the J-adaptive filter for unmodeled accelerations (with $U_{ii} = (5 \times 10^{-4})^2$, $i = 1, 3$; $Q = 0$), the J-adaptive filter for C_L and C_D (with $U_{11} = (1 \times 10^{-2})^2$, $U_{22} = (6 \times 10^{-3})^2$; $Q = 0$), and the extended Kalman filter with the best engineered process noise covariance matrix Q. It should be noted that the J-adaptive filters are not very sensitive to the choice of U. The simulation features radar tracking from nine stations plus onboard accelerations. The radar coverage is indicated in Fig. 4.

Sample position and velocity estimation error time histories for these filters are shown in Figs. 4 and 5. Fine detail of the error structure is not shown in these figures. The peaks in the error curves correspond to skips in the re-entry trajectory and/or tracking data gaps or low elevation angle radar coverage. The

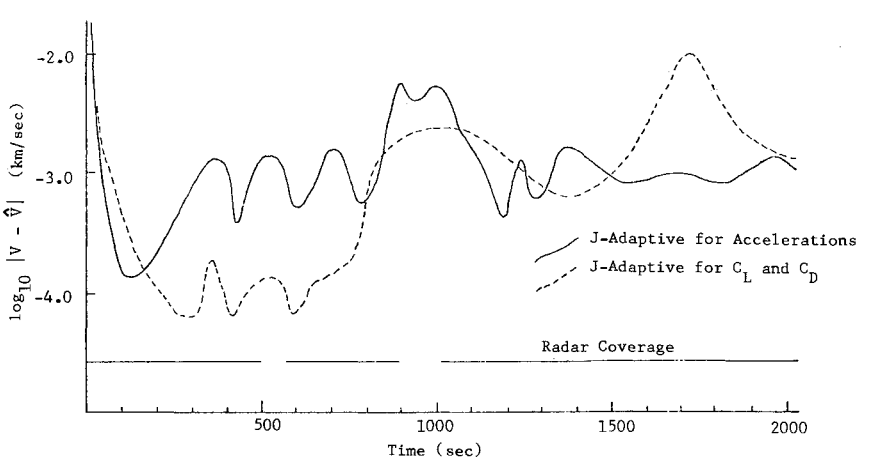

Fig. 5 Velocity estimation errors.

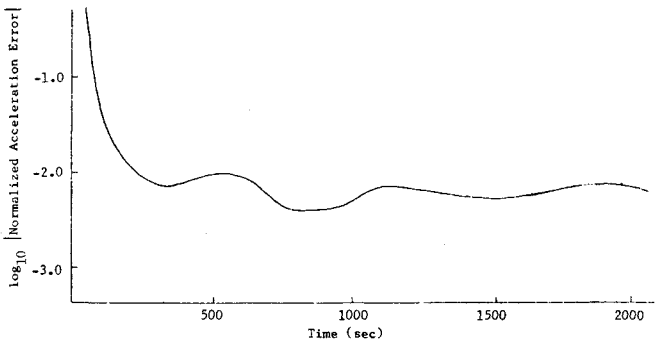

Fig. 6 Normalized acceleration error.

large peak around 1000 sec corresponds to both a skip and a data gap.

Although not shown in the figures, the extended Kalman filter with Q does not track and tends to diverge. It is not easy to engineer a good Q. Furthermore, this filter has a bad numerical feature in the sequential mode. When Q is added in propagation, the covariance matrix P increases; and when data is processed, P decreases. This causes fluctuations of several orders of magnitude in P, tending to cause ill-conditioning and destroying the correlations or the geometry of P.

The J-adaptive filter for C_L and C_D tracks relatively well, except in the regions of the wind gusts (750–950, 1450–1650 sec). Actually, it does not quite recover from the second wind gust. This is because the lift and drag directions span the space of all the model errors with the exception of the winds. As a consequence, this adaptive filter is not adequate in general and needs to be augmented with another variable in the direction orthogonal to lift and drag. It may be noted (see Fig. 5) that, prior to the encounter with the first wind gust, the J-adaptive filter for C_L and C_D tracks extremely well, better than the J-adaptive filter for unmodeled accelerations. This is because (in that region) the first adaptive filter has a better prediction model than the second one.

Figures 4 and 5 indicate that the J-adaptive filter for unmodeled accelerations tracks quite well in the presence of arbitrary model errors, even through the winds. Of course the errors simulated are quite large and this limits the possible tracking accuracy. Tracking accuracy could be improved either by making model errors smaller or giving the filter more tracking data. Toward the end of the trajectory, when multiple station coverage is available, the position and velocity errors almost approach the radar noise level. It may be noted that the onboard accelerations do not substantially improve the estimation when tracking is available. However, during tracking data gaps, onboard accelerations are very useful in inhibiting further error growth. That is to say, the error peaks during tracking data gaps are higher without onboard accelerometer data.

How well the J-adaptive filter for unmodeled accelerations actually tracks these unmodeled accelerations can be seen in Fig. 6. Plotted in this figure is the ratio

$$|a_{\text{observed}} - \hat{a}_{\text{modeled}} - \hat{u}| / |a_{\text{observed}} - \hat{a}_{\text{modeled}}| \qquad (21)$$

where a is the acceleration vector. The denominator in this ratio approximately measures the net acceleration error due to the model errors simulated, while the numerator is the residual acceleration error after using our estimate of the unmodeled acceleration $\hat{u}$. It is seen that the J-adaptive filter identifies 99% of the unmodeled accelerations.

VIII. Conclusions

The results presented appear to have several important and practical implications for re-entry estimation as well as for other estimation problems. First, significant nonlinearities indeed exist in the re-entry estimation problem. The iterated extended Kalman filter appears to offer a practical solution for tracking through nonlinearities without degrading the information content of the data. A practical filter could use this iteration feature when it is appropriate to do so.

The J-adaptive filter concept is sound and shows great promise for practical estimation problems. It can be used to identify models in real time as well as strictly for tracking, as in the unmodeled acceleration mode (Sec. VII). J-adaptive identification of lift and drag coefficients, which may be required for guidance and control, could proceed in the presence of arbitrary model errors by the introduction of a third variable orthogonal to the lift and drag directions. The J-adaptive filter concept is clearly applicable to quite general estimation problems.

IX. References

[1] Wagner, W. E., "Re-Entry Filtering, Prediction and Smoothing," *Journal of Spacecraft and Rockets*, Vol. 3, No. 9, Sept. 1966, pp. 1321–1327.

[2] Jazwinski, A. H., *Stochastic Processes and Filtering Theory*, Academic Press, New York, 1970.

[3] Mehra, R. K., "A Comparison of Several Nonlinear Filters for Reentry Vehicle Tracking," System Control, Inc., Palo Alto, Calif.

[4] Jazwinski, A. H., Pines, S., Hipkins, C., and Flanagan, P., "Nonlinear and Adaptive Estimation Techniques in Reentry," Rept. 72-6, Feb. 1972, Analytical Mechanics Associates, Inc., Seabrook, Md.

[5] Pines, S. and Jazwinski, A. H., "Error Analysis of Space Trajectories," *Proceedings of the Fourth IFAC Symposium on Automatic Control in Space*, International Federation of Automatic Control, Sept. 1971, Dubrovnik, Yugoslavia.